iMRI 2023;27(3);147-153
https://doi.org/10.13104/imri.2023.0004
eISSN 2384-1109

Case Report

Received: February 15, 2023
Revised: March 31, 2023
Accepted: April 14, 2023

Correspondence
Hyungjin Rhee, MD, PhD
Department of Radiology,
Yonsei University
College of Medicine,
50-1 Yonsei-ro, Seodaemun-gu,
Seoul 03722, Korea.
E-mail: hjinrhee@yuhs.ac

An Incidentally Discovered Primary Hepatic Gastrointestinal Stromal Tumor Treated by Surgical Resection and Adjuvant Imatinib Therapy: A Case Report

Sungtae Park[1], Dai Hoon Han[2], Young Nyun Park[3], and Hyungjin Rhee[1]

[1]Department of Radiology, Research Institute of Radiological Science, Center for Clinical Imaging Data Science, Severance Hospital, Yonsei University College of Medicine, Seoul, Korea
[2]Department of Surgery, Severance Hospital, Yonsei University College of Medicine, Seoul, Korea
[3]Department of Pathology, Graduate School of Medical Science, Brain Korea 21 Project, Yonsei University College of Medicine, Seoul, Korea

Gastrointestinal stromal tumors (GISTs) are rare mesenchymal tumors derived from precursors of the interstitial cells of Cajal that commonly arise from the stomach or small intestine. These tumors usually contain *KIT* and/or *PDGFRA* mutations, which encode type III receptor tyrosine kinases. Approximately 10% of GISTs originate from sites other than the gastrointestinal tract, such as the mesentery, urinary bladder, retroperitoneum, pancreas, gallbladder, and liver. These tumors are hypothesized to originate from interstitial Cajal-like cells or undifferentiated pluripotent mesenchymal cells outside the gastrointestinal tract. Primary hepatic GISTs are rare, with most hepatic GISTs being secondary. Here, we report the case of a 69-year-old woman with a rare primary hepatic GIST. The hepatic GIST, measuring 13.5 cm, was incidentally discovered in the right liver lobe and exhibited heterogeneous arterial phase hyperenhancement, washout, diffusion restriction, low signal intensity in the hepatobiliary phase, intratumoral hemorrhage, necrosis, and fluid-fluid levels. Imaging revealed no evidence of extrahepatic primary lesions. GIST was pathologically confirmed via percutaneous biopsy and subsequent surgical resection. Despite adjuvant imatinib therapy, the tumor recurred with peritoneal seeding 15 months postoperatively.

Keywords: Gastrointestinal stromal tumors; Interstitial Cajal-like cell; Magnetic resonance imaging; Gadolinium ethoxybenzyl DTPA; Multidetector computed tomography

INTRODUCTION

Gastrointestinal stromal tumors (GISTs) are rare mesenchymal tumors with an estimated annual incidence of 4.3–22 per million [1]. These tumors usually possess activating oncogene mutations, mostly *KIT* and/or *PDGFRA*, which encode type III receptor tyrosine ki-

nases [2]. GISTs most commonly originate from the gastrointestinal tract, including the stomach (60%–65%), small intestine (20%–25%), rectum (3%–5%), colon (1%–2%), and esophagus (1%) [2]. However, they can also originate from other organs, such as the omentum, mesentery, urinary bladder, retroperitoneum, pancreas, gallbladder, and liver [3]. These tumors, known as extra-gastrointestinal stromal tumors (EGISTs), account for approximately 10% of all GISTs with identifiable primary sites [4]. GISTs originate from precursors of the interstitial cells of Cajal (ICCs). Although the exact carcinogenesis of primary hepatic GIST is yet to be demonstrated, interstitial Cajal-like cells (ICLCs) and ICCs are the probable origins [5]. ICLCs are present in rhythmically active structures such as the heart, urinary bladder, gallbladder, and along the portal vein scaffold and have a similar structure and function as ICCs [6]. Another theory proposes that primary hepatic GISTs originate from ICCs that emerge from undifferentiated pluripotent mesenchymal cells outside the gastrointestinal tract [7]. Herein, we describe a rare case of primary hepatic GIST without any other identifiable primary sites.

CASE REPORT

A 69-year-old woman was referred to Severance Hospital, Seoul, Korea for a liver mass incidentally detected on low-dose chest computed tomography (CT) as part of a routine health check-up. The patient had no medical history except for thyroid cysts and tiny lung nodules (< 1 cm in size) that remained unchanged for > 2 years; thus, they were presumed to be benign. The abdominal mass was asymptomatic. She tested negative for hepatitis B virus surface antigen and hepatitis C virus antibody. Her serum alpha-fetoprotein (5.4 ng/mL), prothrombin induced by vitamin K absence or antagonist-II (13 mAU/mL), carcinoembryonic antigen (0.92 ng/mL), and carbohydrate antigen 19-9 (3.3 U/mL) levels were within the normal range.

The patient underwent liver dynamic CT, which revealed a heterogeneous low-attenuating mass of approximately 13.5 cm involving liver segments 4 and 8 (Fig. 1). The mass showed heterogeneous enhancement in the arterial phase and washout in the portal and delayed phases. The central area of the tumor exhibited no obvious enhancement, suggesting necrosis. Moreover, a small hypoenhancing nodule was identified in liver segment 2 in the portal venous phase. The initial differential diagnoses were cavernous hemangioma and hepatocellular carcinoma (HCC) for large hepatic mass, small hemangioma and intrahepatic metastasis for liver segment 2 lesion.

The patient underwent gadoxetic acid-enhanced liver dynamic magnetic resonance imaging (MRI) for further evaluation (Fig. 2). The MRI revealed a mass measuring approximately 13.5 cm in liver segments 4 and 8 abutting the hepatic capsule. The mass exhibited low signal intensity with focal areas of high signal intensity in the pre-contrast T1-weighted image, suggesting an intratumoral hemorrhage. The mass showed heterogeneous arterial phase hyperenhancement, washout in the portal phase, low signal intensity in the transitional and hepatobiliary phases, and diffusion restriction. The central portion of the tumor was necrotic, with several foci of fluid-fluid levels in the T2-weighted image. A small hypoenhancing nodule in liver segment 2 demonstrated moderately high signal intensity on T2-weighted imaging and diffusion restriction, similar to the large mass. Although the patient was not at high risk of HCC, HCC could not be excluded based on imaging findings; therefore, an ultrasound-guided percutaneous liver biopsy of the large mass was performed. The pathological finding was a malignant spindle cell tumor with diffuse, strong positivity for c-KIT and discovered on gastrointestinal stromal tumor 1 (DOG1) in the tumor cells, which supported the diagnosis of GIST. After the biopsy, the patient underwent positron emission tomography-CT, which showed intense ^{18}F-fluorodeoxyglucose uptake only in the liver mass, with no extrahepatic focal uptake (Fig. 3).

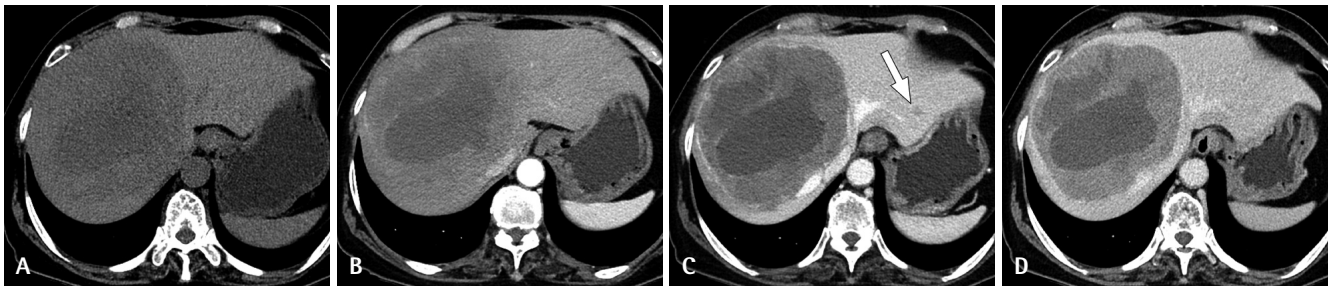

Fig. 1. Liver dynamic computed tomography (CT) image showing two liver masses. Liver dynamic CT scan with precontrast (A), arterial (B), portal (C), and delayed (D) phases. An hepatic mass of approximately 13.5 cm in liver segments 4 and 8 showing hypoattenuation in the precontrast scan (A), heterogeneous enhancement in the arterial phase (B), and washout in the portal (C) and delayed (D) phases. The central area of the tumor exhibits no obvious enhancement in the portal or delayed phases, suggesting necrosis. In addition, a small hypoenhancing nodule in liver segment 2 is detected in the portal phase (C, arrow).

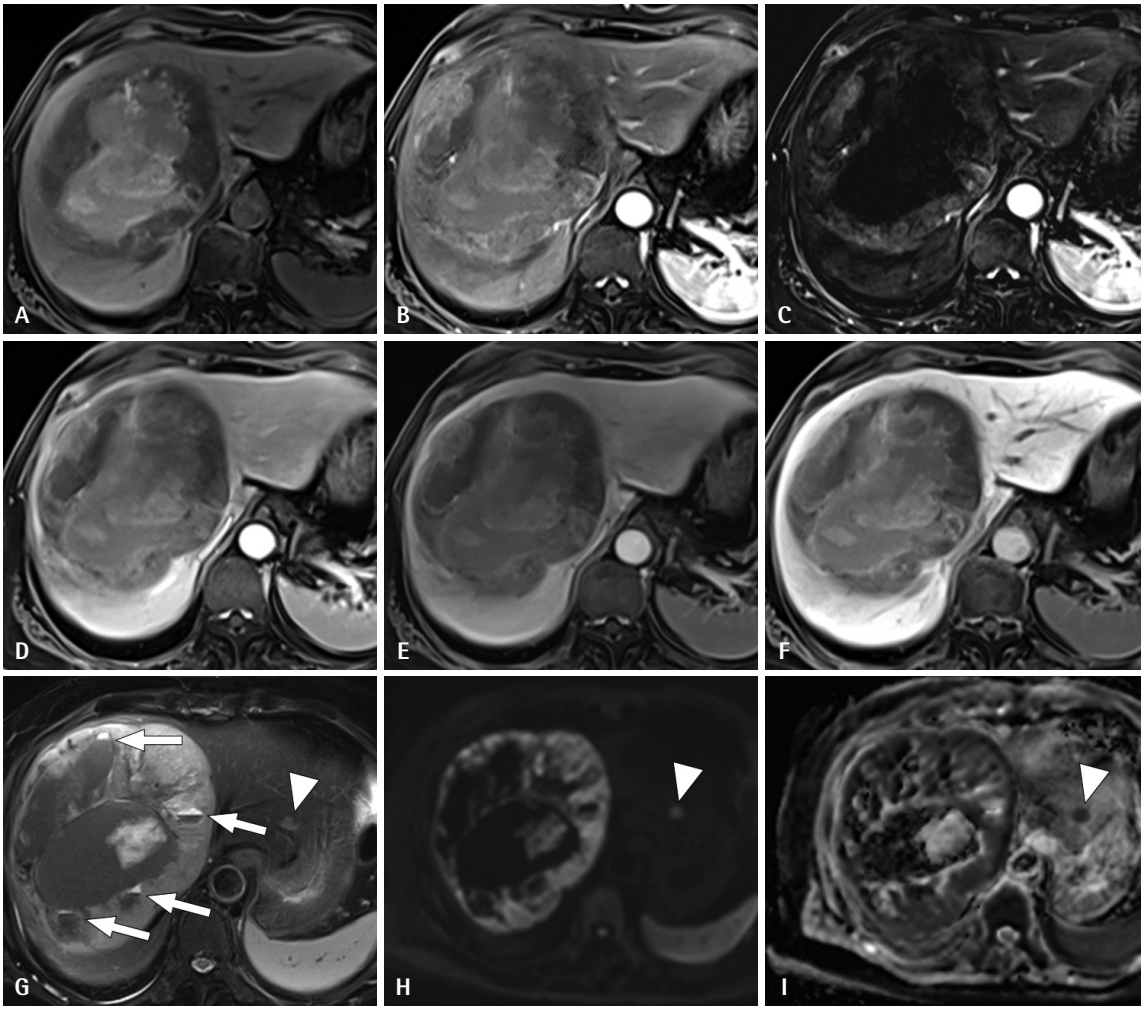

Fig. 2. Gadoxetic acid-enhanced magnetic resonance imaging (MRI) findings of the liver masses. Gadoxetic acid-enhanced MRI with pre-contrast (A), arterial (B), arterial subtraction (C), portal (D), transitional (E), and hepatobiliary (F) phases, T2-weighted images (G), diffusion-weighted images (b = 800 s/mm^2) (H), and apparent diffusion coefficient map (I). The large mass involving liver segments 4 and 8 showed low signal intensity with foci of high signal intensity in the pre-contrast T1-weighted image (A), suggesting focal hemorrhage. The mass shows heterogeneous arterial hyperenhancement (B, C), washout in the portal phase (D), and low signal intensity in the transitional and hepatobiliary phases (E, F). The central area of the large mass is not enhanced, suggesting necrosis. In the T2-weighted image (G), the large mass exhibits its heterogeneous intensity with a central necrotic area and several foci at the fluid-fluid level (arrows). On diffusion-weighted imaging, the mass lesion shows diffusion restriction (H, I). There was another tiny nodular lesion in liver segment 2, with moderate hyperintensity in the T2-weighted image and diffusion restriction (arrowheads) (G-I).

The patient underwent right trisectionectomy and wedge resection of liver segment 2 (Fig. 4). Gross examination of the hepatic tumor revealed a well-demarcated, whitish-to-pinkish multinodular hemorrhagic mass measuring approximately 16.0 × 15.0 × 8.0 cm. The smaller hepatic tumor in liver segment 2 was ill-demarcated and whitish and measured approximately 0.7 × 0.7 × 0.5 cm. The larger mass exhibited diffuse positivity for both c-KIT and DOG1, whereas the smaller tumor exhibited diffuse positivity for c-KIT, supporting the diagnosis of GIST and in line with the previous percutaneous biopsy result. Because no other primary site of GIST was identified, the diagnosis of primary hepatic GIST with a small intrahepatic metastasis in segment 2 was confirmed. The mitotic count of the large tumor was 7 mitoses/50 high-power fields. Tumor size, tumor site, and mitotic count corresponded to those of a high-risk group, according to the 2008 modified National Institutes of Health (NIH) criteria. The patient received adjuvant imatinib therapy (200 mg/day) because of the high-risk features.

Fifteen months after the resection, follow-up abdominal CT revealed possible peritoneal seeding nodules (Fig. 5). All grossly visible seeding nodules were surgically resected and pathologically confirmed as metastatic GIST. The patient received palliative sunitinib treatment (25 mg/day) after metastasectomy and has remained recurrence-free for 9 months.

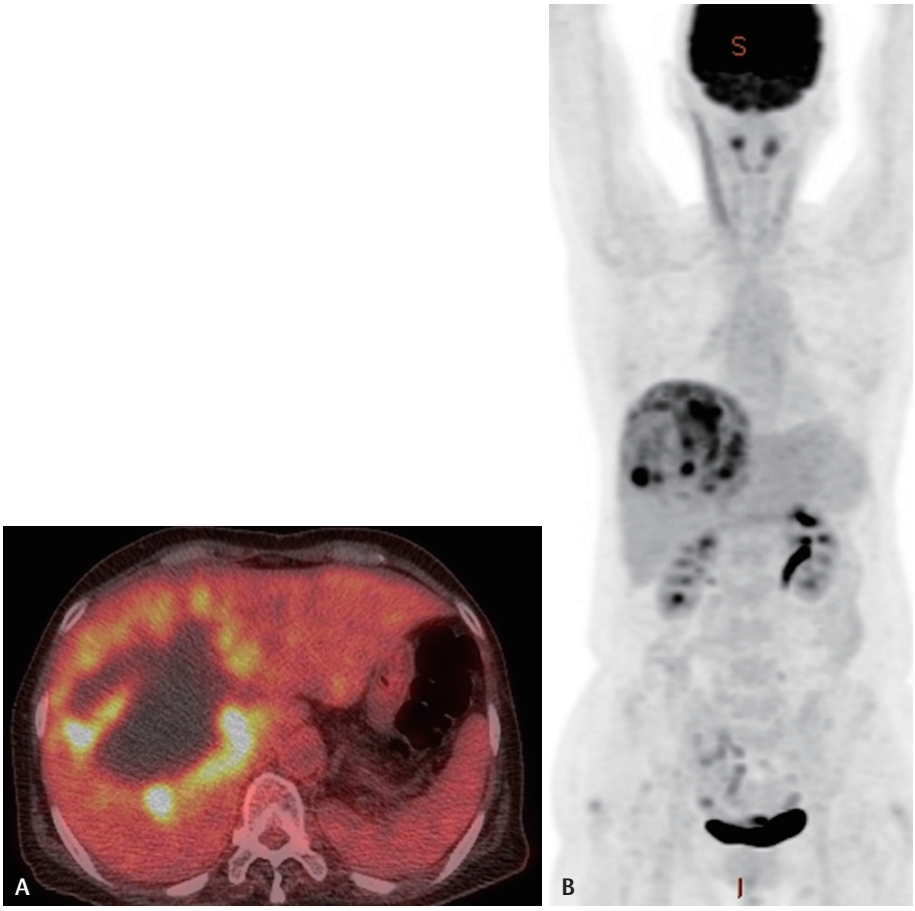

Fig. 3. ^{18}F-fluorodeoxyglucose (^{18}F-FDG) positron emission tomography-computed tomography of the torso. A: High ^{18}F-FDG uptake is noted at the periphery of the liver mass. B: No extrahepatic ^{18}F-FDG focal uptake is observed in the maximal intensity projection image.

DISCUSSION

GIST is the most common mesenchymal tumor of the gastrointestinal tract [1,7]. Because protein expressions of c-KIT and DOG1 are observed in most (> 95%) GISTs, they are considered useful diagnostic markers [7]. GIST can arise anywhere along the gastrointestinal tract, but the most frequent locations are the stomach and small intestine. EGISTs that arise outside the gastrointestinal tract constitute 10% of all GISTs [4]. EGISTs of various origins have been reported, including the mesentery, retroperitoneum, omentum, vagina, pancreas, ovaries, and liver [7]. Primary hepatic GISTs are exceedingly rare, and only 34 cases were reported until 2020 [5].

Considering the rarity of primary hepatic GISTs, limited studies have reported their imaging findings; nonetheless, they exhibit imaging findings similar to those of GISTs in other organs and are typically accompanied by heterogeneous enhancement, necrosis, and cystic changes when the tumor size is large [5]. One case report demonstrated heterogeneous arterial phase hyperenhancement and washout in the delayed phase on CT, and another reported mild heterogeneous arterial phase enhancement and hypoattenuation in the portal and delayed phases [3,8]. Other cases exhibited prolonged uneven enhancement or an entirely cystic appearance [5]. Our case demonstrated mixed solid and cystic tumors with heterogeneous signal intensity, fluid-fluid levels on T2-weighted imaging, and diffusion restriction. Focal T1 hyperintensity was also observed, probably due to the intratumoral hemorrhage. For the dynamic enhancement pattern, focal arterial phase hypervascularity, washout in the portal phase, and non-enhancing necrotic areas until delayed-phase images were observed. Due to the presence of heterogeneous arterial phase hyperenhancement and washout, the possibility of HCC or sarcomatoid HCC was considered. However, given the presence of prominent necrosis and fluid-fluid levels, GIST, neuroendocrine tumor, and undifferentiated embryonal sarcoma are the differential diagnoses. HCC often occurs in high-risk patients (such as those with liver cirrhosis and positivity for hepatitis B virus surface antigen) and is associated with elevated alpha-fetoprotein level. Undifferentiated embryonal sarcoma appears as a multiseptat-

ed cystic lesion due to abundant myxoid stroma causing high signal intensity on T2-weighted imaging [9]. Primary or metastatic neuroendocrine tumors are hypervascular tumors with central necrosis and fluid-fluid levels. Cavernous hemangiomas often demonstrate nodular peripheral and centripetal fill-in; however, the enhancement pattern can vary and occasionally reveal fluid-fluid levels. Bright T2-signal intensity and absence of diffusion restriction are indicative of hemangioma.

Primary hepatic GISTs generally show poorer prognosis than gastric or small intestinal GISTs because of their larger size, higher mitotic index, and subsequent higher NIH risk category, thus requiring adjuvant chemotherapy. One study comparing 11 primary hepatic GISTs and 356 gastric or small intestinal GISTs reported two GIST-related deaths, two recurrences,

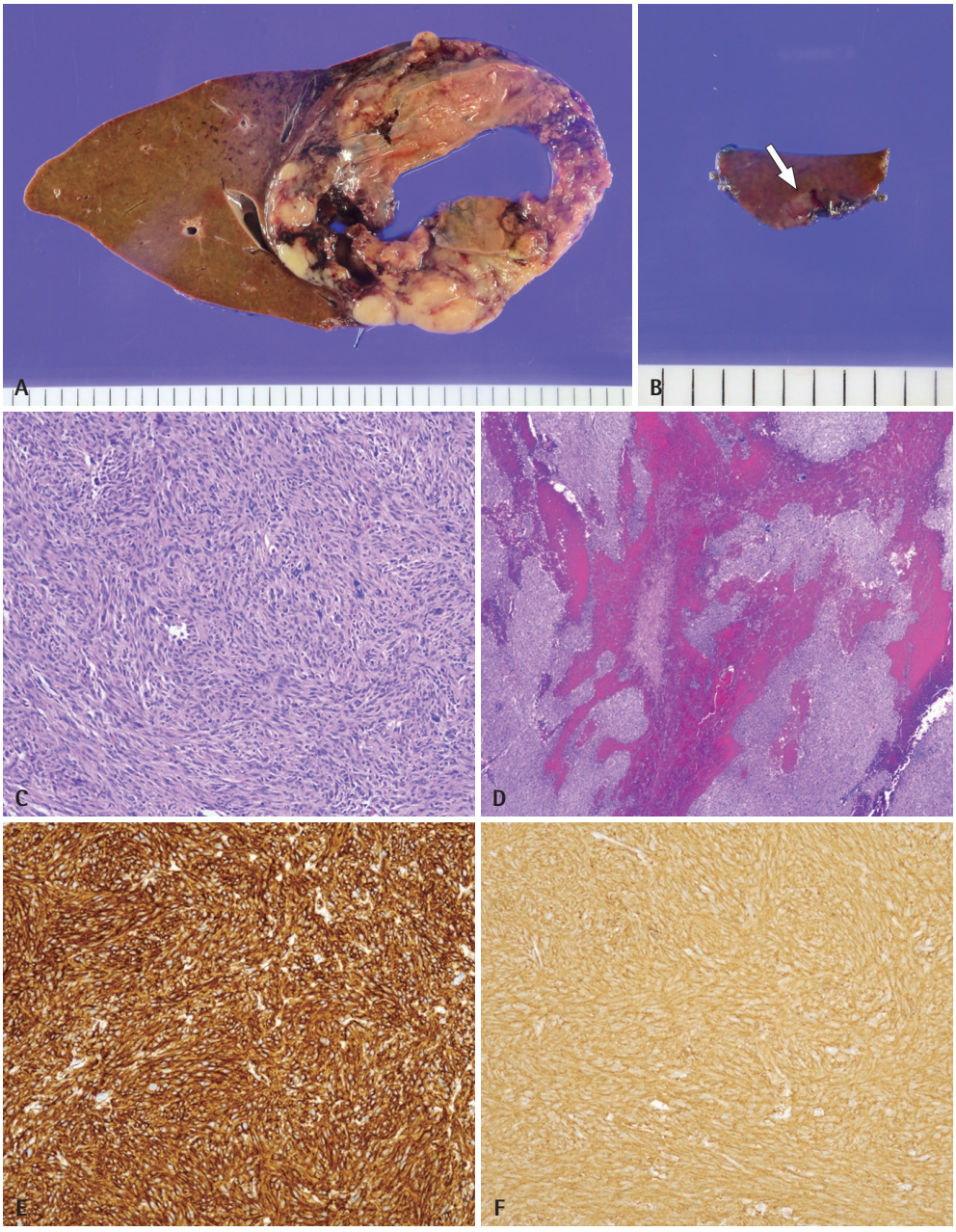

Fig. 4. Gross, histologic, and immunohistochemical findings of the tumor. Gross examination of the hepatic tumors (A, B) revealed a well-demarcated whitish-to-pinkish mass of approximately 16.0 cm with necrosis and hemorrhage in the central portion (A). B: Another 0.7-cm whitish hepatic tumor (arrow) is observed in liver segment 2. C: The tumors are composed of spindle cells with eosinophilic fibrillary cytoplasm (hematoxylin-eosin staining, ×100). D: Necrosis and hemorrhage are noted in the central portion of the large mass (hematoxylin-eosin staining, ×20). The masses show diffuse positivity for both c-KIT (E, ×100) and discovered on gastrointestinal stromal tumor 1 (DOG1) (F, ×100), supporting the diagnosis of gastrointestinal stromal tumor.

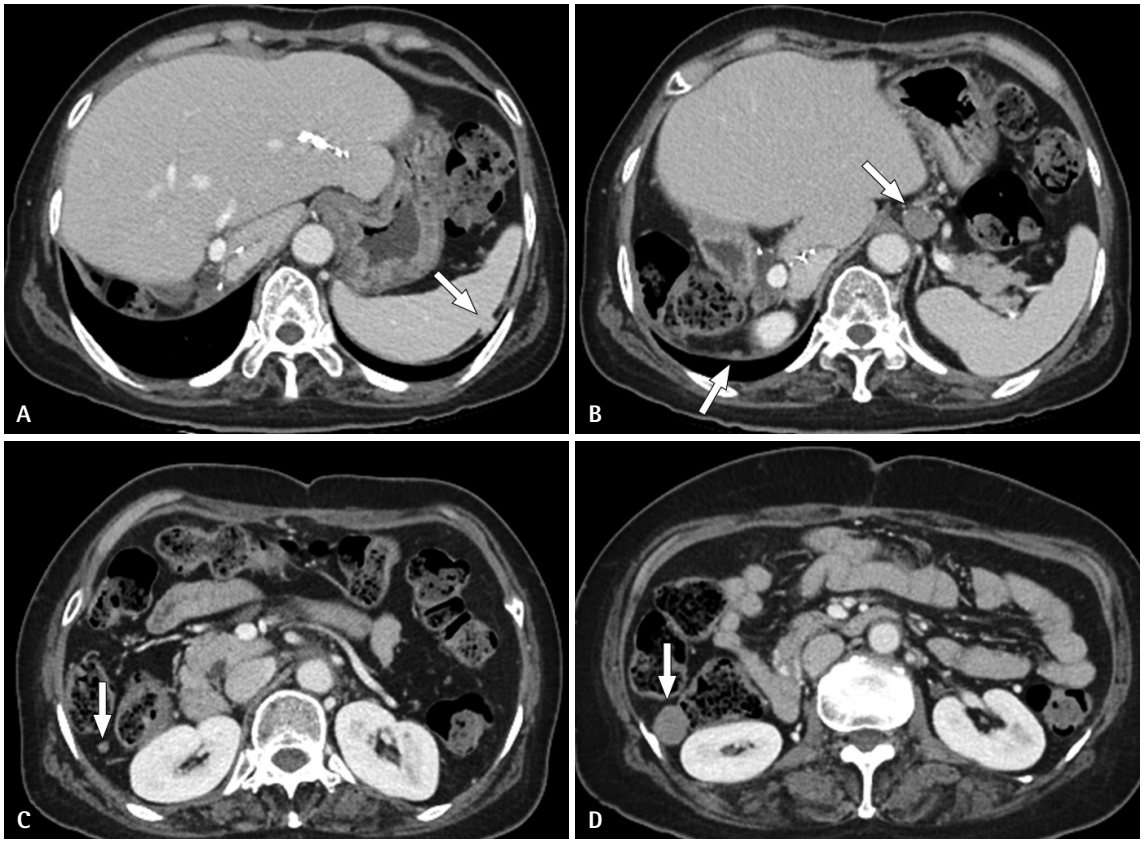

Fig. 5. Abdominal computed tomography 15 months after hepatic resection. Multiple peritoneal seeding nodules are suspected in the peritoneal cavity (arrows): the perisplenic area (A), right subphrenic area, left gastric area (B), and along the right paracolic gutter (C, D).

and two metastases from primary hepatic GISTs during 27.1 months of follow-up, and 33.3% of the 5-year disease-specific survival rates were poorer than those of stomach or small intestinal GISTs [10].

The treatment of primary hepatic GISTs is similar to that of GISTs of other organs of the gastrointestinal tract. As most primary hepatic GISTs belong to the NIH high-risk group, lesion resection and adjuvant tyrosine kinase inhibitor chemotherapy, such as imatinib, are required [5]. Our patient also received adjuvant imatinib therapy after tumor resection because of the high-risk classification. However, peritoneal seeding nodules were detected at 15 months postoperatively. Although the large hepatic mass abutted the hepatic capsule, there was no gross evidence of tumor rupture on imaging. Microscopic rupture of the tumor or iatrogenic peritoneal dissemination during percutaneous biopsy or hepatic resection could be potential causes of peritoneal seeding metastasis after surgery. Primary hepatic GISTs tend to grow rapidly and may cause rupture or bleeding, which may necessitate transarterial embolization. Radiofrequency or microwave ablation can be performed for small tumors. In the case of resistance to tyrosine kinase inhibitors, liver transplantation may improve survival [5].

In conclusion, we present a rare case of a primary hepatic GIST that was discovered incidentally, which was confirmed by surgical resection and recurred despite adjuvant imatinib therapy. Although primary hepatic GISTs show various radiological findings and are rare, radiologists should consider the possibility of primary hepatic GIST in patients with hypervascular hepatic masses, no risk factors of HCC, and normal level of serum markers for HCC.

Ethics Statement

This study was approved by the Institutional Review Board of Severance Hospital, Seoul, Korea, and the requirement for patient consent was waived (No. 4-2022-1571).

Availability of Data and Material

Data sharing not applicable to this article as no datasets were generated or analyzed during the study.

Conflicts of Interest

Hyungjin Rhee, a contributing editor of the *Investigative Magnetic Resonance Imaging*, was not involved in the editorial evaluation or decision to publish this article. All remaining authors have declared no conflicts of interest.

Author Contributions

Conceptualization: Hyungjin Rhee. Data curation: Sungtae Park, Hyungjin Rhee. Funding acquisition: Hyungjin Rhee. Investigation: all authors. Supervision: Hyungjin Rhee. Writing—original draft: Sungtae Park, Hyungjin Rhee. Writing—review & editing: all authors.

ORCID iDs

Sungtae Park https://orcid.org/0000-0002-5264-5551
Dai Hoon Han https://orcid.org/0000-0003-2787-7876
Young Nyun Park https://orcid.org/0000-0003-0357-7967
Hyungjin Rhee https://orcid.org/0000-0001-7759-4458

Funding Statement

This study was supported by a grant from the National Research Foundation of Korea (NRF) funded by the Korean government (MSIT) (No. RS-2023-00208307).

REFERENCES

1. Søreide K, Sandvik OM, Søreide JA, Giljaca V, Jureckova A, Bulusu VR. Global epidemiology of gastrointestinal stromal tumours (GIST): a systematic review of population-based cohort studies. Cancer Epidemiol 2016;40:39-46.
2. Blay JY, Kang YK, Nishida T, von Mehren M. Gastrointestinal stromal tumours. Nat Rev Dis Primers 2021;7:22.
3. Nadkarni S, Patkar S, Acharya MR, et al. Primary hepatic gastrointestinal stromal tumour (GIST): unusual presentation and diagnosis. J Gastrointest Cancer 2020;51:1061-1064.
4. Du CY, Shi YQ, Zhou Y, Fu H, Zhao G. The analysis of status and clinical implication of KIT and PDGFRA mutations in gastrointestinal stromal tumor (GIST). J Surg Oncol 2008;98:175-178.
5. Qian XH, Yan YC, Gao BQ, Wang WL. Prevalence, diagnosis, and treatment of primary hepatic gastrointestinal stromal tumors. World J Gastroenterol 2020;26:6195-6206.
6. Rusu MC, Pop F, Hostiuc S, Curcă GC, Streinu-Cercel A. Extrahepatic and intrahepatic human portal interstitial Cajal cells. Anat Rec (Hoboken) 2011;294:1382-1392.
7. Yi JH, Park BB, Kang JH, et al. Retrospective analysis of extragastrointestinal stromal tumors. World J Gastroenterol 2015;21:1845-1850.
8. Fernandes MR, Ghezzi CLA, Grezzana-Filho TJ, et al. Giant hepatic extra-gastrointestinal stromal tumor treated with cytoreductive surgery and adjuvant systemic therapy: a case report and review of literature. World J Gastrointest Surg 2021;13:315-322.
9. Crider MH, Hoggard E, Manivel JC. Undifferentiated (embryonal) sarcoma of the liver. Radiographics 2009;29:1665-1668.
10. Liu Z, Tian Y, Liu S, et al. Clinicopathological feature and prognosis of primary hepatic gastrointestinal stromal tumor. Cancer Med 2016;5:2268-2275.